JOURNAL OF THERMOPHYSICS AND HEAT TRANSFER
Vol. 9, No. 4, October–December 1995

Adaptive Finite Element Method for Mixed Convection

D. Pelletier* and F. Ilinca†
École Polytechnique de Montréale, Montreal, Quebec H3C 3A7, Canada

This article presents an adaptive remeshing finite element method to solve heat transfer problems by mixed convection. Solutions are obtained in primitive variables using a high-order finite element approximation on unstructured grids. Two general estimators are developed for analyzing finite element solutions to planar and axisymmetric mixed convection heat transfer problems. The methodology is applied to heat transfer predictions for two cases of practical interest.

Nomenclature

a = radius of the tube
c_p = specific heat
e = error
f = friction coefficient
Gr = Grashoff number
$\boldsymbol{g}$ = gravity vector
h = element size
k = thermal conductivity
Nu = Nusselt number
$\boldsymbol{n}$ = outward unit vector
p = pressure
q = heat flux
Re = Reynolds number
Ri = Richardson number
T = temperature
$\boldsymbol{u}$ = velocity vector
v, s, w = test functions
β = volume expansion coefficient
δ = element size for new mesh
η = relative error
μ = viscosity
ρ = density
τ = stress tensor
∇ = gradient operator
$\nabla\cdot$ = divergence

Subscripts
av = average
e = entry value
h = finite element solution
m = mean value
∂, B = boundary
∞ = infinity value
0 = reference value

Introduction

HEAT transfer by mixed convection is of practical significance for many systems of engineering interest. Examples include heat exchangers, cooling processes in nuclear reactors, combustors and furnaces, and cooling of electronic equipment. All these problems are characterized by the interaction of buoyancy forces and forced convection that often results in recirculation zones that may not be attached to solid walls or sharp corners. This contrasts sharply with more familiar forced convection problems. All mixed convection situations present the same challenge for computational methods: the location and extent of shear layers and stagnation point is very difficult to determine a priori. The net result is that achieving accurate solutions is a very demanding task for the analyst.

Adaptive finite element methods (FEMs) provide a powerful approach for accurately solving such complex problems. Grids points are automatically clustered in the region of rapid solution variation to improve accuracy. In the present approach this is done in such a way as to result in a solution that is uniformly accurate throughout the flow domain. This tight control on the solution process makes it possible to obtain "numerically exact solutions" to the Navier–Stokes equations. The adaptive process turns out to be cost-effective in the sense that the best numerical solution is obtained at the least computational cost.

While initial breakthroughs occurred nearly seven years ago in compressible aerodynamics,[1] little work has been done for incompressible flows and even less for heat transfer problems. Proof of concept computations were reported in Refs. 2 and 3. In Refs. 4–9, the methodology proposed by the authors was quantitatively validated by solving flows with known analytical solutions and by computing cases for which experimental measurements were available. Cases treated covered isothermal laminar flows, heat transfer by free convection, conjugate heat transfer with variable fluid properties, and turbulent free shear flows. This article presents a rigorous extension of the methodology to mixed convection.

Adaptive FEMs have been demonstrated for forced and free convection problems. In the former case the momentum equation is decoupled from the energy equation, while in the latter one the Boussinesq term is the driving force of the flow. Mixed convection flows present special challenges because they give rise to complex flow patterns, especially with localized heating or cooling of the wall: flow reversal away from the wall and recirculation zones on the centerline of a pipe. These unusual phenomena are due to the interaction of a forced flow with Boussinesq effects. This gives rise to thin layers or slender recirculation bubbles whose location is difficult to predict a priori and which may have a significant impact on pressure drop and heat transfer.[10] It is far from obvious that adaptive methods targeted at forced or free convection are adequate for mixed convection. This article is focused on determining whether the adaptive remeshing procedure is suitable for such flow problems.

This article is organized as follows: first the equations of motion and the finite element solver are reviewed. The meth-

Presented as Paper 94-0347 at the AIAA 32nd Aerospace Sciences Meeting and Exhibit, Reno, NV, Jan. 10–13, 1994; received Feb. 21, 1994; revision received Feb. 24, 1995; accepted for publicaton Feb. 27, 1995.

*Professor, Mechanical Engineering Department, Centre de Recherche en Calcul Appliqué and Génie Mécanique, P.O. Box 6079, Station Centre-Ville. Member AIAA.

†Graduate Research Assistant, Mechanical Engineering Department, Centre de Recherche en Calcul Appliqué and Génie Mécanique, P.O. Box 6079, Station Centre-Ville.

odology section describes the two error estimators and the adaptive remeshing strategy. The method is then applied to the prediction of heat transfer for two problems of practical interest: mixed convection in vertical pipe and in a sudden expansion. Results are compared to experiments. This article closes with conclusions.

Modeling of the Problem

Equations of Motion

The flow is modeled by the Navier–Stokes, continuity, and energy equations with the Boussinesq approximation:

$$\begin{aligned} \rho \boldsymbol{u}\cdot\nabla\boldsymbol{u} &= -\nabla p + \nabla\cdot\tau + \rho g\beta(T - T_0) \\ \nabla\cdot\boldsymbol{u} &= 0 \\ \rho c_p \boldsymbol{u}\cdot\nabla T &= \nabla\cdot q \end{aligned} \tag{1}$$

where the stress tensor τ is defined by

$$\tau = \mu\{\nabla\boldsymbol{u} + (\nabla\boldsymbol{u})^T\} \tag{2}$$

and $q = k\nabla T$ is the heat flux. Appropriate boundary conditions complete the statement of the problem.

Finite Element Solver

The variational equations solved by the FEM are obtained by multiplying the above equations by appropriate test function and integrating over the domain of interest. Application of the divergence theorem to the momentum and temperature diffusion terms leads to the following weak form:

$$\begin{aligned} &(\rho\boldsymbol{u}\cdot\nabla\boldsymbol{u}, v) + a(\boldsymbol{u}, v) - (p, \nabla\cdot v) - (\rho g\beta T, v) \\ &\quad = -(\rho g\beta T_0, v) + \langle\hat{t}, v\rangle \\ &(s, \nabla\cdot\boldsymbol{u}) = 0 \\ &(\rho c_p \boldsymbol{u}\cdot\nabla T, w) + \mathrm{d}(T, w) = \langle q_B, w\rangle \end{aligned} \tag{3}$$

where

$$a(\boldsymbol{u}, v) = \int_\Omega \tau(\boldsymbol{u}):\nabla v \, \mathrm{d}\Omega \tag{4}$$

$$\mathrm{d}(T, w) = \int_\Omega q(T)\cdot\nabla w \, \mathrm{d}\Omega \tag{5}$$

and the boundary terms are given by

$$\langle\hat{t}, v\rangle = \int_{\partial K\setminus\Gamma_i} (\tau\cdot\boldsymbol{n} - p\boldsymbol{n})\cdot v \, \mathrm{d}s + \int_{\partial K\cap\Gamma_i} \hat{t}\cdot v \, \mathrm{d}s \tag{6}$$

$$\langle q_B, w\rangle = \int_{\partial K\setminus\Gamma_q} q\cdot\boldsymbol{n} w \, \mathrm{d}s + \int_{\partial K\cap\Gamma_q} q_B w \, \mathrm{d}s \tag{7}$$

These variational equations are solved by a standard Galerkin method coupled to an augmented Lagrangian algorithm to treat the incompressibility.[11] The equations are discretized using the seven-node triangular element that uses an enriched quadratic velocity field, a quadratic temperature, and a linear discontinuous pressure approximation.[4,7]

Adaptive Methodology

The basic idea behind adaptive methods is to assess the quality of an initial solution obtained on a coarse mesh by using some form of error estimation and to modify the structure of the numerical approximation in a systematic fashion so as to improve the overall quality of the solution. There are several ways of achieving adaptivity: P-methods increase the degree of the polynomial approximation[12]; R-methods relocate grid points,[13] and H-methods proceed by either mesh enrichment or remeshing.[1,3,4]

A variant of an H-method, called adaptive remeshing, has been retained because it provides control of element size and grading to accurately resolve flow features such as shear and thermal layers. In this method the problem is first solved on a coarse grid to roughly capture the physics of the flow. The resulting solution is then analyzed to determine where more grid points are needed and an improved mesh is generated. The problem is solved again on the new mesh using the solution obtained on the coarser mesh as an initial guess. This process is repeated until the required level of accuracy is achieved.

Remeshing also offers an elegant and simple approach to use the best proven finite element approximations in an adaptive context.[11,14] This circumvents the problem associated with P-methods of satisfying the so-called Ladyshenskaya–Babuška–Brezzi (LBB) compatibility condition between the velocity and pressure approximations. It also eliminates the "hanging node problem" encountered in some H-refinement methods.[3]

Error Estimation

This section describes two error estimation techniques for assessing the accuracy of the solutions obtained by the finite element solver.

Projection Error Estimator

This technique was first introduced in Ref. 15 and is based on the observation that the derivatives of the finite element solution are discontinuous on the element boundary while the exact derivatives are continuous. The difference between the two is a measure of the accuracy of the numerical solution. However, the exact solution is not known in cases of practical interest, but because of the superconvergence property of the FEM, an approximation to the true derivatives can be obtained by a least-squares projection of the finite element derivatives:

$$\sum_{K\in T}\left\{\int_K \phi_m(\tau_{ij} - \tilde{\tau}_{ij}) \, \mathrm{d}x\right\} = 0 \tag{8}$$

where

$$\tilde{\tau}_{ij} = \sum_{i=1}^{7} \phi_n\{\tilde{\tau}_{ij}\}_n \tag{9}$$

is the projection of the FEM stresses τ into the space of the velocity interpolation functions. The nodal values of the continuous stresses are then obtained by solving the following system:

$$\left[\sum_{K\in T}\int_K \phi_m\phi_n \, \mathrm{d}x\right]\{\tilde{\tau}_{ij}\}_n = \left\{\sum_{K\in T}\int_K \phi_m\tau_{ij} \, dx\right\} \tag{10}$$

The same least-squares projection approach is used to obtain a continuous approximation for the pressure and heat fluxes. The velocity, pressure, and temperature contributions to the error are then given by

$$\begin{aligned} e^u &= \tilde{\tau} - \tau \\ e^p &= \tilde{p} - p \\ e^T &= \tilde{q} - q \end{aligned} \tag{11}$$

where the "~" denotes a least-squares projection.

The combined norm of the velocity, pressure, and temperature fields and their errors are computed using the following expressions:

$$\begin{aligned} \|(\boldsymbol{u}, p, T)\| &= \{\|\boldsymbol{u}\|_E^2 + \|p\|_0^2 + \|T\|^2\}^{1/2} \\ \|(e^u, e^p, e^T)\| &= \{\|e^u\|_E^2 + \|e^p\|_0^2 + \|e^T\|^2\}^{1/2} \end{aligned} \tag{12}$$

where the individual norms are defined as

$$\|\boldsymbol{u}\|_E^2 = \int_\Omega \tau : \tau \, d\Omega, \qquad \|e^u\|_E^2 = \int_\Omega e^u : e^u \, d\Omega$$
$$\|p\|_0^2 = \int_\Omega |p|^2 \, d\Omega, \qquad \|e^p\|_0^2 = \int_\Omega |e^p|^2 \, d\Omega \tag{13}$$
$$\|T\| = \int_\Omega q \cdot q \, d\Omega, \qquad \|e^T\|^2 = \int_\Omega e^T \cdot e^T \, d\Omega$$

This is the so-called natural norm induced by the variational formulation of the problem, which includes variations of the fluid properties. This ensures that mesh refinement will occur in regions where heat fluxes and shear stresses variations are significant. It will avoid over-refinement in cases where temperature and velocity may have steep gradient but fluid properties are small enough such that heat fluxes and stresses show little variation.

Local Partial Differential Equation Problem for the Error

This approach provides an estimate of the error without having to solve the global least-squares problems required by the previous estimator. Partial differential equations (PDEs) and their weak forms for the velocity, pressure, and temperature errors can be derived directly from the Navier–Stokes equations[5,16,17] by substituting the following relationship:

$$\begin{aligned} \boldsymbol{u} &= \boldsymbol{u}_h + e^u \\ p &= p_h + e^p \\ T &= T_h + e^T \end{aligned} \tag{14}$$

where the subscript h denotes the finite element solution, and e^x is the error in the variable x. Unsubscripted quantities are the exact solution.

The following variational equations for the error are obtained:

$$\begin{aligned} a(e^u, v) - (e^p, \nabla \cdot v) + (\rho g \beta e^T, v) &= -a(\boldsymbol{u}, v) \\ + (-\rho u_h \cdot \nabla u_h - \rho g \beta (T_h - T_\infty), v) + (p_h, \nabla \cdot v) \\ + \langle [\tau \cdot \boldsymbol{n} - p_h \boldsymbol{n}]_A, v \rangle_{\partial K \setminus \Gamma_i} + \langle \hat{t}, v \rangle_{\partial K \cap \Gamma_i} \\ (s, \nabla \cdot e^u) &= (s, \nabla \cdot u_h) \\ d(e^T, w) = (-\rho c_p u_h \cdot \nabla T_h, w) - d(T_h, w) \\ + \langle q_B, w \rangle_{\partial K \cap \Gamma T} + \langle [q_h \cdot \boldsymbol{n}]_A, w \rangle_{\partial k \setminus \Gamma_q} \end{aligned} \tag{15}$$

The terms in parentheses on the right-hand side (RHS) represent the element residuals, a measure of the accuracy of the finite element solution inside an element. The terms in brackets are the average momentum and heat fluxes across element faces. The difference between this average value and the raw flux evaluated on the face of the element reflects how well the solutions on two neighboring elements are matched. The second equation is a measure of mass conservation.

This is a well-posed Neumann problem that is discretized locally on each element. The Neumann conditions are given by the viscous and conduction fluxes. Zero Dirichlet conditions are applied to the error components on the element faces along solid walls. Velocity and temperature errors are approximated with three quartic bubble functions associated to the midside nodes of the triangle. The pressure error is approximated with a quadratic bubble function. This results in small 10 by 10 systems of equations that are inexpensive to solve. The norm of the errors is computed as in the previous section. Further theoretical details may be found in Refs. 17 and 18.

Adaptive Remeshing

There remains one key issue to discuss: how does one exploit the knowledge of the error distribution to design a better mesh. The adaptive remeshing strategy is straightforward and follows that proposed in Refs. 1, 4, and 5, and proceeds as follows:

```
1 - Generate an initial mesh
2 - Compute the finite element solution
3 - Compute error estimate
4 - if ( global error < tolerance ) then
        - stop
    else
        - compute grid density from error estimate
        - generate an improved mesh according to grid
          density
        - interpolate current solution on new mesh
      - goto 2
    end if
```

We now provide details on some of the steps of this algorithm.

The success of the adaptive strategy depends entirely on the adequate determination of the grid density function. It must ensure that smaller elements are generated in regions of large errors and bigger triangles will be created where the mesh is too fine. Once the finite element solution has been obtained, the error on each element is computed using one of the previously described estimators. The global norms of the solution and the error are computed as follows:

$$\|e_{\text{tot}}\|^2 = \sum \|e_k\|^2 \tag{16}$$

so that the relative error can be evaluated

$$\eta = \|e_{\text{tot}}\| / \|U\| \tag{17}$$

There remains to compute the element size for the improved mesh so that elements are smaller in regions of large error and bigger in regions where the solution is already accurate. This is achieved by requiring that the improved mesh be optimal (i.e., that all elements have the same average error e_{av}). Now, given a target relative error η_t, the total and target average error can be related as follows:

$$\|e_{\text{av}}\| = \eta_t (\|U\| / \sqrt{n}) \tag{18}$$

Finally, an expression for element sizes can be derived from the asymptotic rate of convergence of the finite element approximation that relates the error to some power k of the element size h:

$$\|e\| = ch^k \tag{19}$$

which can also be written for the target error:

$$\|e_{\text{av}}\| = c\delta^k \tag{20}$$

(k equals 2 for the present case). These two equations can be solved for the required element size:

$$\delta = [\eta_t \|U\| / \|e\| \sqrt{n}]^{1/k} h \tag{21}$$

This distribution of element size is then used as the grid function in an advancing front mesh generator in order to generate an improved mesh.

This strategy can be used in either of two modes. In the fixed relative error mode η_t is kept fixed at say 5 or 10%. In the reduction mode the target error $\|e_{\text{av}}\|$ is set equal to a fraction of $\|e_{\text{tot}}\|$ computed on the current mesh. The fixed relative error target mode works best when only velocity gra-

dients appear in the norms. For many problems a target relative error of 1–5% is quite acceptable for engineering applications.[15] It was found that the error reduction mode works best when different variables appear in the error estimate, as is the case here in Eq. (12). A 10-fold reduction of the error estimator usually yields results that are "grid converged."

Theoretical analysis for the seven-node triangle clearly indicates that the convergence rate with mesh refinement is optimal and equal to two for both the L_2 norm of the velocity gradients and the L_2 norm of pressure [i.e., the norms used in Eq. (12)]. This is important because it leads to a quasioptimal remeshing algorithm. Using a rate of convergence other than this one leads to over- or under-refinement of the mesh. Furthermore, the theory presented in Ref. 19 results in a combined rate of convergence for all dependent variables. Any other choice leads to a different rate of convergence for each variable, which makes it impossible to determine a unique and consistent mesh size.

Application

Mixed Convection in Vertical Pipe

This configuration was studied experimentally and numerically in Ref. 10. Figure 1 presents a sketch of the domain with boundary conditions. Calculations were performed with a nondimensional form of the equations. The nondimensional variables are defined as follows:

$$x_i = x_i^*/a, \qquad u_i = u_i^*/u_m$$
$$\mu = 1/Re, \qquad \theta = (T - T_h)/(T_e - T_h) \tag{22}$$

where a is the radius of the pipe, u_m is the mean velocity, Re is the Reynolds number $Re = (\rho a u_m)/\mu$, T_h is the temperature of the heated/cooled section, and T_e is the inlet temperature.

The simulation was performed for the two cases of Ref. 10. For the first case (A) the Reynolds number is 25, the Grashoff is 5000, and the dimensionless temperature on the top wall is 4. The conditions result in massive separation on the cold wall, followed by rapid acceleration of the flow on the strongly heated upper section of the wall. This in turn results in a recirculation zone at the center of the pipe. For the second case (B) the test section is heated and the top wall is cooled to the inlet temperature. The values of the parameters in this case are $Re = 50$, $Gr = -50{,}000$, and $\theta_\infty = 1$.

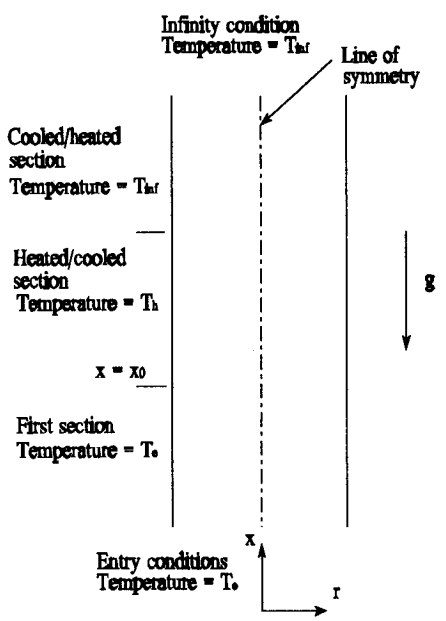

Fig. 1 Mixed convection in vertical pipe: computational domain and boundary conditions.

Table 1 Vertical pipe, projection estimator

Mesh	No. of nodes	No. of elements	Solution norm	Error estimate
0	847	378	117.0	1.069×10^{-1}
1	1922	905	116.8	3.077×10^{-2}
2	3658	1733	115.2	1.542×10^{-2}
3	7328	3561	115.5	6.566×10^{-3}

Table 2 Vertical pipe, local problem estimator

Mesh	No. of nodes	No. of elements	Solution norm	Error estimate
0	847	378	117.0	9.660×10^{-2}
1	1650	779	117.0	6.893×10^{-2}
2	3264	1573	117.3	2.715×10^{-2}

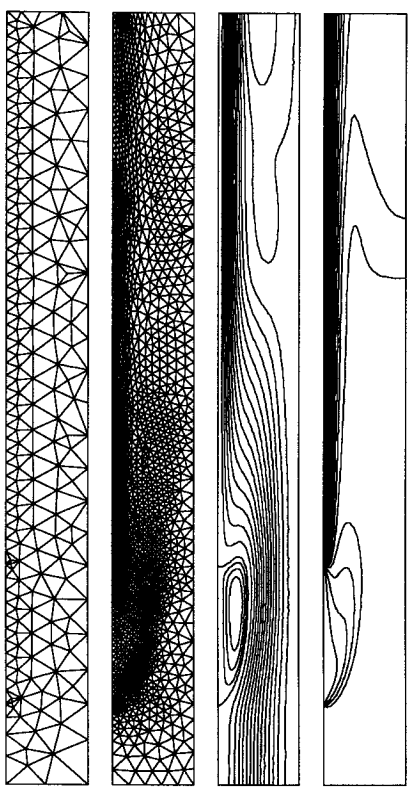

Fig. 2 Mixed convection in a vertical pipe: case A.

The computations were performed by using both the postprocessing and local problem error estimators. The behavior of the adaptive process for case A is presented in Tables 1 and 2. Both estimators produce the reduction of the error at each cycle. Hence, the solution accuracy improves steadily at each adaptation cycle. Note that in both cases the meshes, solution and error norms behave similarly. Nearly identical results were obtained with both methods. Hence, only one set of results is presented.

Figure 2 presents the initial mesh, the final mesh, streamlines, and temperature contours for the final solution on the case A. All plots show smooth contour lines. The mesh has been highly refined along the strongly heated top wall because of the thin hydrodynamic and thermal boundary layers. This is to be expected since the heating of the top wall greatly reduces the density of the fluid and results in a strong acceleration of the flow.

On case B the flow is very strong accelerated in the central heated section near the wall, having recirculation zones on

the center of the pipe and near the cooled wall. As can be seen on Fig. 3 grid points are concentrated in regions having high velocity and temperature gradients. The adaptive strategy results in an efficient deployment of computational grid points to achieve a good accuracy. Temperature contours and streamlines obtained on the final mesh are also plotted in Fig. 3.

The predictions for the local and average Nusselt numbers and for the skin friction coefficient are compared with the numerical results of Ref. 10. The Nusselt number is defined as $Nu = hL/k$ and expressed in terms of θ leads to[10]

$$Nu = -\left.\frac{\partial\theta}{\partial R}\right|_{R=1} \Big/ (\theta_m - \theta|_{R=1}) \tag{23}$$

where θ_m is the average temperature. The average Nusselt number for a point x is defined by

$$Nu_{\mathrm{Av}} = \frac{1}{x - x_0}\int_{x_0}^{x} Nu(x)\,dx \tag{24}$$

where x_0 represent the coordinate at the beginning of the heated/cooled region.

According with Ref. 10 we calculate also the friction coefficient times the Reynolds number as $Ref = 8\Omega|_{R=1}$, where Ω denotes the vorticity:

$$\Omega = \left(\frac{\partial u}{\partial r}\right)_w \tag{25}$$

The values obtained on the first and the adapted meshes, together with the predictions from Ref. 10 are plotted on Fig. 4. As can be seen, adaptation results in very accurate predictions of these derived quantities. Differences observed for the average Nusselt number when compared to those of Ref. 10 are due to the different numerical values of the initial point of integration. The Nusselt number at the initial point x_0 is theoretically infinite because of the discontinuity in the temperature. Hence, the result of the integration depends on the first element size, close to x_0. Consequently, the value of the average Nusselt number is precise to an additive constant. Similar results are obtained for case B as shown on Fig. 5.

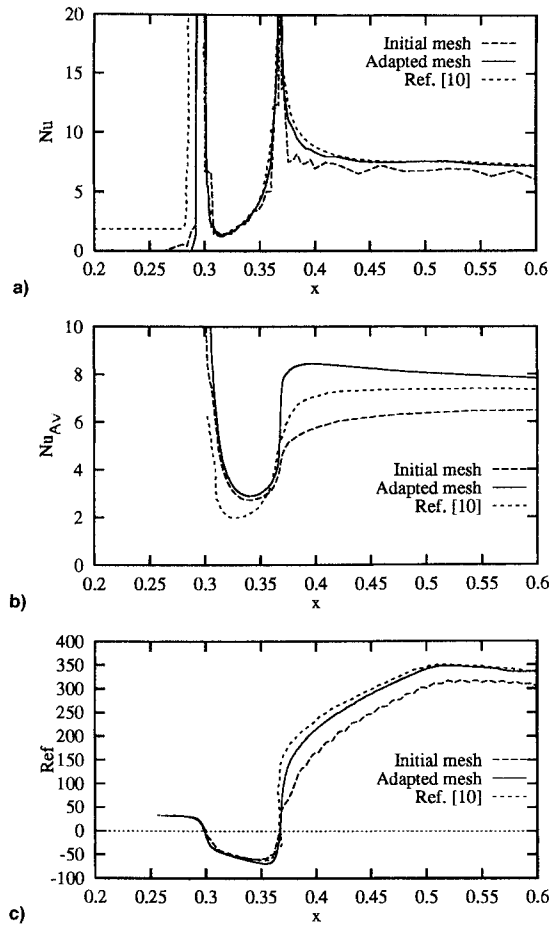

Fig. 4 Case A: a) local Nusselt number, b) average Nusselt number, and c) friction coefficient times Reynolds number.

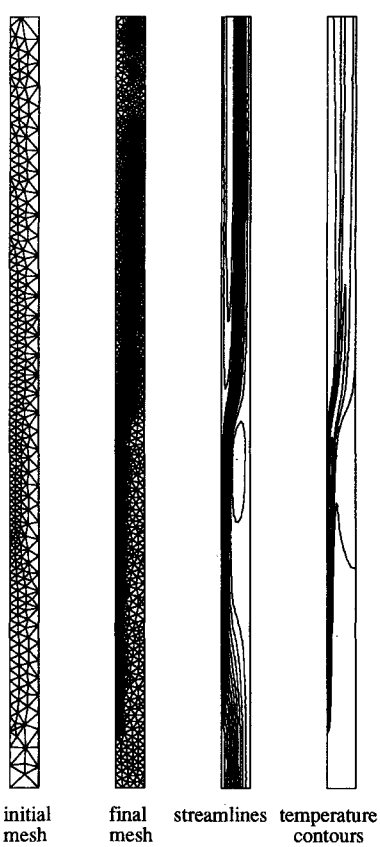

Fig. 3 Mixed convection in a vertical pipe: case B.

Mixed Convection with Transverse Injection in a Sudden Expansion

The configuration studied in Ref. 20 is shown on Fig. 6. Laminar flow enters the backward facing step whose bottom walls and step (2, 3, 5 on Fig. 6) are heated at constant temperature. The top wall is adiabatic and fluid can be injected with a velocity v_j at the base of the step through an opening (4 on Fig. 6). Simulations were performed at a Reynolds number of 100 and $Ri = 0.4$. This case is more challenging than the simple isothermal flow over a backward-facing step because buoyancy forces act perpendicularly to the main flow direction. Fluid is injected vertically at the base of the step with a velocity $v_j = 0.2\bar{U}$, where $\bar{U}$ is the mean velocity at the channel inflow. The effect of the Boussinesq term results in a thermal layer all along the bottom wall. The behavior of the adaptive process for both error estimators is presented in Tables 3 and 4. At each cycle the error is reduced by a factor that is very close of the imposed value of 3. Hence, the solution accuracy improves steadily at each adaptation cycle. As can be seen, both estimators behave similarly. Error estimates, solution norms, and mesh characteristics are comparable.

Figure 7 shows the meshes that were adaptively generated by using the postprocessing error estimator. Nearly identical results are obtained with the local problem error estimator. Hence, only one set of results is presented. As can be seen

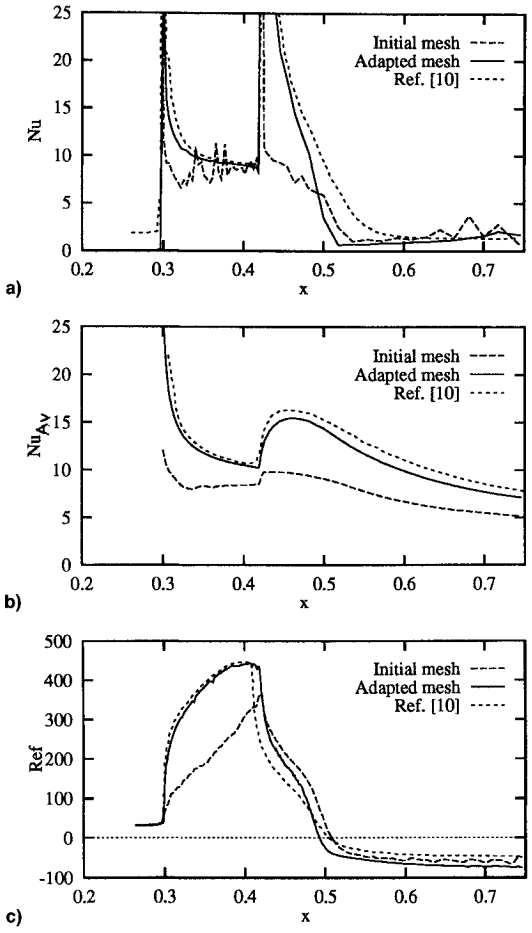

Fig. 5 Case B: a) local Nusselt number, b) average Nusselt number, and c) friction coefficient times Reynolds number.

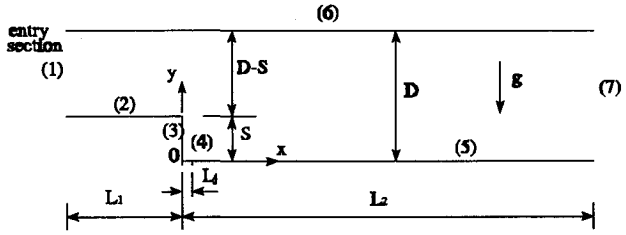

Fig. 6 Mixed convection in a sudden expansion: computational domain and boundary conditions.

refinement occurs near the corner, near the injection point, and on the base of the step where fluid injection causes a thin wall shear layer. Isotherms show the significant cooling effect due to injection. The apparently excessive refinement near the outflow boundary is due to the simple boundary conditions used in the present computations, which does not include the effect of the buoyancy forces at the outflow boundary. Isotherms and streamlines plotted on Fig. 8 agree very well with those of Ref. 20. Figure 9 presents the Nusselt number distribution on the base of the step. As can be seen, injection significantly enhances heat transfer on the backward-facing wall.

Computational Efficiency

These results illustrate the improved resolution that can be achieved with adaptivity. The proposed adaptive strategy also results in a cost-effective solution algorithm that is well worth the added complexity. Table 5 contains computational statistics obtained on an IBM E/S 9000 with vector facility, for mixed convection in the sudden expansion with cold fluid injection, using the projection estimator. Timings, in seconds, include all aspects of computations (grid generation, flow solution, error estimation, and interpolation of the solution between grids).

Computation of the error estimate represents typically less than 20% of the cost of obtaining a solution on a given mesh. Complete solution of this problem required a total of 620 CPU seconds. Solving the same problem directly on the final mesh without using intermediate grids would have required approximately 780 CPU seconds. Our computing time of 10 min on an IBM E/S 9000 should be contrasted with the 360–480 min on a Vax 8650 for a comparable grid.[20] This is a

Table 3 Mixed convection in a sudden expansion, projection estimator

Mesh	No. of nodes	No. of elements	Solution norm	Error estimate
0	778	347	1.127	4.944×10^{-2}
1	1451	668	1.099	1.984×10^{-2}
2	3132	1481	1.088	8.211×10^{-3}
3	7270	3497	1.087	3.569×10^{-3}

Table 4 Mixed convection in a sudden expansion, local problem estimator

Mesh	No. of nodes	No. of elements	Solution norm	Error estimate
0	778	378	1.127	5.712×10^{-2}
1	1422	661	1.099	1.949×10^{-2}
2	3121	1481	1.092	8.725×10^{-3}
3	7018	3497	1.087	3.596×10^{-3}

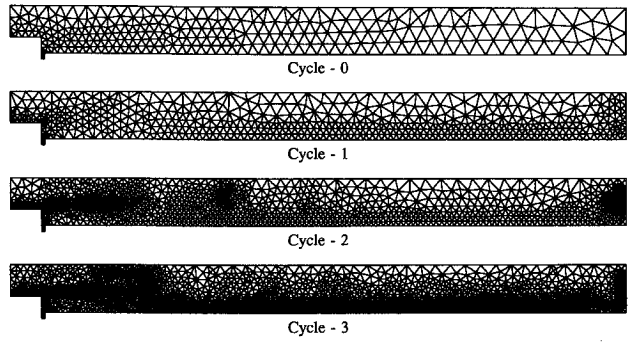

Fig. 7 Mixed convection with injection: adapted meshes.

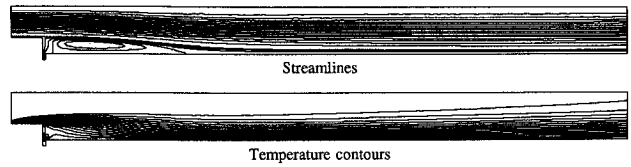

Fig. 8 Mixed convection with injection: solution on the final mesh.

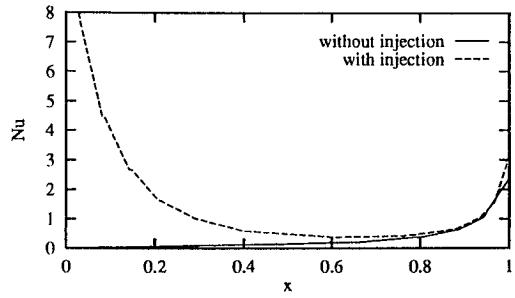

Fig. 9 Nusselt number distribution on the step.

Table 5 Computational statistics for adaptation

Cycle	No. of interpolations	Meshing, s	Solution, s	Adaptation, s
0	9	1.44	37.83	7.65
1	3	4.93	38.28	16.51
2	3	10.49	123.36	37.44
3	3	19.76	258.29	65.96

significant improvement even when differences in hardware speed are taken into account.

It should also be noted that without adaptivity it would have been nearly impossible to generate a grid leading to comparable accuracy without at least doubling the number of grid points on the final mesh. In fact, it is very difficult to achieve a good allocation of grid points without the extra knowledge gained from the error estimates. Given that Gaussian elimination is used at each Newton iteration, the increase in computational cost is proportional to the cube of the number of grid points. It follows that nonadaptive computations of comparable accuracy would have been far more expensive than adaptive ones.

Conclusions

An adaptive remeshing finite element procedure has been presented for solving mixed convection heat transfer problems. The two error estimators presented have proven reliable and convergent when compared with experimental measurements. Both estimators are sensitive to hydrodynamic and thermal layers. The adaptive procedure has shown robust and can be used effectively in a blackbox fashion with little or no intervention on the part of the user. Predictions for heat transfer agree well with previous experimental and numerical observations.

Acknowledgment

The authors would like to acknowledge the financial support of NSERC and FCAR. We thank Éric Turgeon and Frédéric Tran-Khanh for their assistance in producing some of the numerical results.

References

[1]Peraire, J., Vahdati, M., Morgan K., and Zienkiewicz, O. C., "Adaptive Remeshing for Compressible Flows," *Journal of Computational Physics*, Vol. 72, No. 2, 1987, pp. 26–37.

[2]Wu, J., Zhu, J. Z., Szmelter J., and Zienkiewicz O. C., "Error Estimation and Adaptivity in Navier-Stokes Incompressible Flows," *Computational Mechanics*, Vol. 6, No. 3, 1990, pp. 259–270.

[3]Wang, K. C., and Carey, G. F., "Adaptive Grids for Coupled Viscous Flow and Transport," *Computational Methods in Applied Mechanics and Engineering*, Vol. 82, No. 2, 1990, pp. 365–383.

[4]Hétu, J. F., and Pelletier, D., "Adaptive Remeshing for Viscous Incompressible Flows," *AIAA Journal*, Vol. 30, No. 8, 1992, pp. 1986–1992.

[5]Hétu, J.-F., and Pelletier, D., "A Fast Adaptive Finite Element Scheme for Viscous Incompressible Flows," *AIAA Journal*, Vol. 30, No. 11, 1992, pp. 2677–2682.

[6]Pelletier, D., and Hétu, J.-F., "An Adaptive Finite Element Methodology for Incompressible Viscous Flows," *Advances in Finite Elements for Fluid Dynamics II, Proceedings of the ASME Winter Annual Meeting* (Anaheim, CA), 1992, pp. 1–12 (FED-137).

[7]Pelletier, D., Hétu, J.-F., and Ilinca, F., "An Adaptive Finite Element Method for Convective Heat Transfer," *AIAA Journal*, Vol. 32, No. 4, 1994, pp. 741–747.

[8]Pelletier, D., Ilinca, F., and Hétu, J.-F., "An Adaptive Finite Element Method for Turbulent Free Shear Flow Past a Propeller," *AIAA Journal*, Vol. 32, No. 11, 1994, pp. 2186–2193.

[9]Pelletier, D., Ilinca, F., and Hétu, J.-F., "An Adaptive Finite Element Method for Convective Heat Transfer with Variable Fluid Properties," *Journal of Thermophysics and Heat Transfer*, Vol. 8, No. 4, 1994, pp. 687–694.

[10]Morton, B. R., Ingham, D. B., Keen, D. J., and Heggs, P. J., "Recirculating Combined Convection in Laminar Pipe Flow," *Journal of Heat Transfer*, Vol. 111, Feb. 1989, pp. 106–113.

[11]Pelletier, D., and Fortin, A., "Are FEM Solutions of Incompressible Flows Really Incompressible? (or How Simple Flows Can Cause Headaches)," *International Journal for Numerical Methods in Fluids*, Vol. 9, No. 1, 1989, pp. 99–112.

[12]Zienkiewicz, O. C., Gago, J. P., and Kelley, D. W., "The Hierarchical Concepts in Finite Element Analysis," *Computers and Structures*, Vol. 16, No. 1, 1983, pp. 53–65.

[13]Lohner, R., Morgan, K., and Zienkiewicz, O. C., "Adaptive Grid Refinement for the Euler and Compressible Navier-Stokes Equations," *Accuracy Estimates and Adaptive Refinement in Finite Element Computations*, edited by I. Babuska, O. C. Zienkiewicz, J. P. Gago, and E. R. de A. Oliveira, Wiley, New York, 1986, pp. 281–298.

[14]Fortin, M., and Fortin, A., "Experiments with Several Elements for Incompressible Flows," *International Journal for Numerical Methods in Fluids*, Vol. 5, No. 9, 1985, pp. 911–928.

[15]Zienkiewicz, O. C., and Zhu, R. J. Z., "A Simple Error Estimator and Adaptive Procedure for Practical Engineering Analysis," *International Journal for Numerical Methods in Engineering*, Vol. 24, No. 2, 1987, pp. 337–357.

[16]Hétu, J. F., "Méthode d'Éléments Finis Adaptatives pour les Écoulements Visqueux Incompessibles," Ph.D. Dissertation, École Polytechnique de Montréale, Montreal, Canada, Dec. 1991.

[17]Oden, J. T., Demkowicz, L., Strouboulis, T., and Devloo, P., "Adaptive Methods in Solid and Fluid Mechanics," *Accuracy Estimates and Adaptive Refinement in Finite Element Computations*, Wiley, New York, 1986.

[18]Oden, J. T., "The Best FEM," Finite Element in Analysis and Design 7, 1990, pp. 103–114.

[19]Cuvelier, C., Segal, A., and Van Steenhoven, A. A., "Finite Element Methods and Navier-Stokes Equations," D. Reidel Publishing, Dordrecht, Holland, The Netherlands, 1986.

[20]Soong, C. Y., and Hsueh, W. C., "Mixed Convection in a Suddenly-Expanded Channel with Effects of Cold Fluid Injection," *International Journal of Heat and Mass Transfer*, Vol. 36, No. 6, 1993, pp. 1477–1484.